INTEGRATED CONTROL TO THE BIPED WALKING ROBOT

João Bosco Gonçalves
Department of Electrical Engineering, University of Taubaté
Rua Daniel Danelli, s/n – CEP 12060-440, Taubaté, São Paulo, Brazil.
jb.goncalves@universiabrasil.net

Douglas Eduardo Zampieri
Department of Computational Mechanics
School of Mechanical Engineering
CP   : 6122, State University of Campinas
CEP. 13083-970, Campinas, São Paulo, Brazil.
douglas@fem.unicamp.br

Abstract. The main objective of this work is to present and discuss some results obtained from our project and implementation of an integrated control system for a biped robot machine in the dynamic gait. We divided the integrated control system in two sub-systems: a control of the trajectories for the legs and an automatic generator of trajectory for the trunk, which updates the conditions of position and speed for the trunk, from the evolution of the legs.

Keywords: biped robot machine, dynamic gait, trajectory of the trunk

1. Introduction

Basically, there are two major research areas in biped walking robot: the static gait and the dynamic gait. The static gait is characterized when the biped walking robot has the ground projection of its global center of mass (GCoM) within the foot-support area (support polygon or stability region). In this case, the localization of the center of pressure (CoP) is identical to the GCoM. Otherwise, the dynamic gait is characterized when the GCoM leaves the support polygon, but the CoP falls within the foot-support area (Goswami, 1999). When the GCoM is in front of the CoP, their distance provides a measure of stability which defines the static threshold of stability[1]. Existing inertial and gravitational forces, this distance adds torques that cause turns around the CoP and the possible fall of the biped walking robot.

To assure the dynamic gait it is necessary to implement a dynamic control for the biped walking robot. The challenge is to endow the biped walking robot with a trunk (inverted pendulum) whose trajectory is planned to compensate torques inherent to the walking dynamic. Since the inertial and gravitational forces are considered, the dynamic modeling of the trunk considers the dynamic interaction between the inferior members and the trunk, establishing a system of non-linear equations whose input is the trajectories of the legs. If the trajectories of the inferior members are planned, the trunk's trajectory can be determined (Li et al., 1992).

The main objective of this work is to present and discuss some results obtained from our project and implementation of an integrated control system for a biped walking robot in the dynamic gait. We divided the integrated control system in two sub-systems: a control of the trajectories for the legs and an automatic generator of trajectory for the trunk, which updates the conditions of position and speed for the trunk, from the evolution of the legs.

2. Biped Robot Machine

We conceived our prototype of the biped walking robot by using the Solidworks® software (Predabon, E. and Bocchese, C., 2003), whose basic philosophy was to elaborate a three-dimensional prototype, divided in subsystems properly joined to impose the restrictions of the relative movements. The physical parameters (mass, volume, moments of inertia, etc) of the prototype are calculated automatically, from the characteristics of the materials to be used, from the forms, geometric dimensions and coordinate systems.

The biped walking robot comprises **7** links (two ankles, two lower legs, two upper legs and a hip) interconnected by **10** revolute joints, which constitute the legs. Solidary to the hip there is an inverted pendulum, with **2** perpendicular revolute joints that allow a three-dimensional pendulum movement. Figure 1 illustrates the biped walking robot. The Cartesian coordinates systems were distributed by employing Denavit and Hartemberg's rules. In this case, links and joints are marked in a systematic way.

---

[1] This technical term is used in aeronautics area.
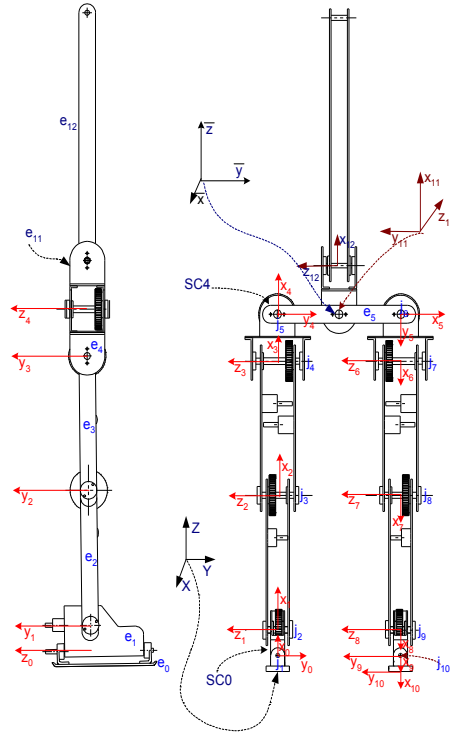
Figure 1. Biped walking robot.

Table 1 presents the information about the physical parameters of the model. The nth link has its moment of inertia computed in relation to the nth Cartesian system, located in the corresponding center of mass. The crossed moments of inertia are null.

Table 1. The physical parameter of the biped walking robot.

	Length	Mass, kg	Moments of inertia, kg m².			Center of Mass, m.			%	Coordinates system
	$\times 10^{-3}$	$\times 10^{-2}$	$\times 10^{-3}$			$\times 10^{-2}$			$\times 10^{-2}$	
Link-j	e_j	m_j	I_{11}	I_{22}	I_{33}	x_C	y_C	z_C	m_j/MT	
0	36	51	4	4	0	-2	0	-4	335	SC0
1	61	93	3	1	3	-1	0	0	610	SC1
2	316	88	1	9	9	-7	0	0	577	SC2
3	316	112	2	11	10	-9	0	-1	735	SC3
4	110	98	3	3	3	-3	0	-2	643	SC4
5	316	65	8	2	6	0	0	-1	427	XYZ
6	110	98	3	3	3	3	0	2	643	SC5
7	316	112	2	11	10	9	0	1	735	SC6
8	316	88	1	9	9	7	0	0	577	SC7
9	61	93	3	1	3	1	0	0	610	SC8
10	36	51	4	4	0	2	0	4	335	SC9
11	680	575	0	430	430	52	-2	-1	3773	XYZ
Total Mass, MT		152 4								

3. Dynamic Model

We considered the biped walking robot as a mechanism in an open chain. By using the formalism of Denavit-Hartemberg to describe its kinematics characteristics, we derived the inverse kinematics and the dynamic modeling. For

the dynamic modeling, the software Maple® V (Keith, G. et al., 1997) was used to implement the formularization of Newton-Euler (Craig, 1995), which permitted the automation of the process of symbolic modeling (acronym NEROBOT). The basic data necessary to use the program NEROBOT are: the parameters of Denavit-Hartemberg, the moments of inertia, the mass, and the center of mass of each link. The result is a dynamic model in the matrix form, given in Eq. (1).

$$[D]\{\ddot{\theta}(t)\}+\{C(\dot{\theta}(t),\dot{\theta}(t))\}+\{G(\theta(t))\}+\{F(\dot{\theta}(t))\}=\{\tau(t)\}-\{M(t)\}-\{\Delta(t)\} \tag{1}$$

Where:

[D]	Matrix mass;
{C}	Coriolis e centripetal forces vector;
{G}	Gravitational forces vector;
{F}	Dissipative forces vector;
{τ}	External forces vector;
{M}	External moment vector;
{Δ}	Generalized forces of reaction vector between hip and trunk;
{θ}	Angular position vector.

We consider the biped walking robot as two subsystems: the legs and the trunk (inverted pendulum). The interaction between the subsystems is caused by the generalized forces of reaction in the joint between the trunk and the hip, which is caused by their relative movements. Thus, we admit that the dynamics of the mounted inverted pendulum on a car in movement represents the main characteristics of coupling between these subsystems.

Using the NEROBOT, we obtained the dynamic model of the legs, presented in the literal form, due to the complexity and the great extension of its model. For simplifications we considered {M} = 0 in Eq. (1), resulting Eq. (2).

$$[D]\{\ddot{\theta}\}+\{C(\dot{\theta},\dot{\theta})\}+\{G(\theta)\}+\{F(\dot{\theta})\}=\{\tau\}-\{\Delta\} \tag{2}$$

By using the NEROBOT, a dynamic model for the trunk was derived, according to Eq. (3) and Eq. (4).

$$d_{11}{}^0\ddot{z}_5 + b_1\left({}^0\dot{z}_5\right) = -d_{13}\ddot{\theta}_{12} - c_1\left(\theta_{11},\dot{\theta}_{12}\right) \tag{3}$$

$$\begin{bmatrix} d_{22} & 0 \\ 0 & d_{33} \end{bmatrix}\begin{Bmatrix} \ddot{\theta}_{11} \\ \ddot{\theta}_{12} \end{Bmatrix}+\begin{Bmatrix} c_2(\theta_{11},\dot{\theta}_{12}) \\ c_3(\theta_{11},\dot{\theta}_{12}) \end{Bmatrix}+\begin{Bmatrix} h_2(\theta_{11},\theta_{12}) \\ h_3(\theta_{11},\theta_{12}) \end{Bmatrix}+\begin{Bmatrix} f_2(\dot{\theta}_{11}) \\ f_3(\dot{\theta}_{12}) \end{Bmatrix}=\begin{Bmatrix} \tau_2 \\ \tau_3 \end{Bmatrix}-\begin{Bmatrix} 0 \\ d_{13}{}^o\ddot{z}_5 \end{Bmatrix} \tag{4}$$

Where:

$$d_{11} = m_5 + m_{11} + m_{12} \qquad d_{12} = 0 \qquad d_{13} = -m_{12}(a_{12}+L)c_3 \tag{5}$$

$$d_{22} = m_{12}\left\{\frac{1}{2}\left[c_{2q_3}\left(a_{12}^2+La_{12}+L^2+I_y\right)+a_{12}^2+L^2+I_y\right]+2a_{11}c_3(L+a_{12})+La_{12}\right\}+a_{11}^2(m_{11}+m_{12}) \tag{6}$$

$$d_{23} = 0 \tag{7}$$

$$d_{33} = m_{12}\left\{a_{12}(2L+a_{12})+L^2\right\}+I_z \tag{8}$$

$$c_1 = m_{12}c_3(a_{12}+L)\dot{q}_3^2 \tag{9}$$

$$c_2 = -m_{12}\left\{s_{2q_3}\left(L^2+a_{12}^2+2La_{12}+I_y\right)+2a_{11}s_3(L+a_{12})\right\}\dot{q}_2\dot{q}_3 \tag{10}$$

$$c_3 = m_{12}\left[s_{2q_3}\left(La_{12}+\frac{I_y}{2}+\frac{a_{12}^2}{2}+\frac{L^2}{2}\right)+s_3a_{11}(L++a_{12})\right]\dot{q}_3^2 \tag{11}$$

$$h_2 = -\left\{a_{11}s_2(m_{11}+m_{12})+m_{12}c_2c_3(a_{12}+L)\right\}g \tag{12}$$

$$h_3 = -m_{12}s_2s_3(a_{12}+L)g \tag{13}$$

Analyzing Eq. (3) and Eq. (4) we can conclude that the terms of the left and of the right side of Eq. (3) are related to the dynamic of the legs of the biped walking robot and to the generalized forces of reaction vector, respectively. The generalized forces of reaction vector are the disturbances to the movement of the biped walking robot. Similarly, the terms of the left and the right side of the Eq. (4) are related to the dynamic of the inverted pendulum and to the generalized forces of reaction vector (which is considered a disturbance to the movement of the inverted pendulum), respectively. So, Eq. (3) and Eq. (4) show the influences of the movements of the dynamic legs in the movement of the inverted pendulum and vice-versa.

4. Integrated Control System

The integrated control system is formed by two subsystem controls: the first, which uses feedback linearization and adaptive control approach and, the second which is an automatic generator of trajectories of the trunk. Similarly to the control of the trajectories of the legs, the trajectories of the trunk are controlled by the computed torque technique (Craig, 1995) whose control law possesses the terms of the nominal model of the robot, the reference model and the uncertainties. Neural networks using radial basis functions (RBF) provide the on-line identification of the uncertainties. The automatic generator of the trajectories of the trunk uses a recurrent neural network (RNN) that manipulates the positions and velocities of the legs to compute the positions for the trunk, based on the zero moment point (ZMP) criterion. Figure 2 illustrates the proposed scheme for the integrated control system.
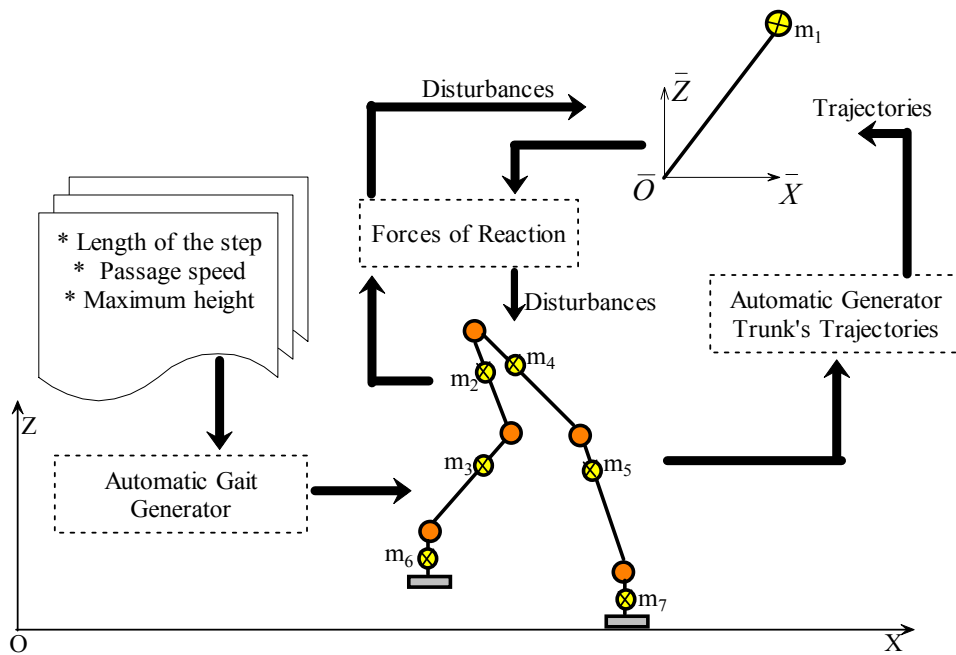
Figure 2. Scheme for the Integrated Control System.

4.1 Feedback linearization and the adaptive control approach

4.1.1 Project of the Reference Model

One can consider a second-order reference model, whose locations of the poles in the complex plan agree with the project specifications, so that the servomechanism simulates the analogous behavior of the standard second-order systems (GE, et. al. 1998). This control technique is similar to the supervised learning. The reference model provides the desired patterns (targets) for the input (references trajectories). The desired patterns are compared with the respective measured variables of the biped walking robot. The error between the desired patterns and the measured variables is used to adjust the parameters of the compensator and of the model of the plant.

By considering a second-order model for each degree of freedom, Eq. (14) represents the reference model in the state space form.

$$\{\dot{\underline{\Omega}}\} = [\underline{A}]\{\dot{\underline{\Omega}}\} + [\underline{B}]\{u\} \tag{14}$$

Where:

$$[\underline{A}] \overset{\Delta}{=} \begin{bmatrix} [0]_{n\times n} & [I]_{n\times n} \\ [A_2]_{n\times n} & [A_1]_{n\times n} \end{bmatrix} \qquad \text{Matrix associated to the states vector, } \in \Re^{2n\times 2n}; \tag{15}$$

$$[\underline{B}] \overset{\Delta}{=} \begin{bmatrix} [0]_{n\times n} \\ -[A_2]_{n\times n} \end{bmatrix} \qquad \text{Matrix associated to the source vector, } \in \Re^{2n\times 2n}; \tag{16}$$

$$\{\underline{\Omega}\} \overset{\Delta}{=} \begin{Bmatrix} \{\theta\} \\ \{\dot{\theta}\} \end{Bmatrix} \qquad \text{State vector, } \in \Re^{2n}; \tag{17}$$

$$[A_1] = -\begin{bmatrix} 2\zeta_1\omega_1 & 0 & 0 \\ 0 & \ddots & 0 \\ 0 & 0 & 2\zeta_n\omega_n \end{bmatrix} \qquad \begin{array}{l} \text{Diagonal matrix with } n \text{ products between } \zeta \\ \text{(damping factor) e } \omega \text{ (natural frequency)} \end{array} \tag{18}$$

$$[A_2] = -\begin{bmatrix} \omega_1^2 & 0 & 0 \\ 0 & \ddots & 0 \\ 0 & 0 & \omega_n^2 \end{bmatrix} \qquad \text{Diagonal Matrix with } n \text{ natural frequency } (\omega), \text{ rad/s}; \tag{19}$$

4.1.2 Project of the Adaptive Control System

Equation (20) represents a biped walking robot in the state space form, in which, to simplify the notation, the dependence of the angular variable was suppressed.

$$\{\dot{\Omega}\} = [A]\{\Omega\} + [B][D]^{-1}(\{\tau\} + \{\Gamma\} - \{\Delta\}) \tag{20}$$

Where:

$$[A] \overset{\Delta}{=} \begin{bmatrix} [0]_{n\times n} & [I]_{n\times n} \\ [0]_{n\times n} & [0]_{n\times n} \end{bmatrix} \qquad \text{Matrix associated to the state vector, } \in \Re^{2n\times 2n}; \tag{21}$$

$$[B] \overset{\Delta}{=} \begin{bmatrix} [0]_{n\times n} \\ [I]_{n\times n} \end{bmatrix} \qquad \text{Matrix associated to the source vector, } \in \Re^{2n\times n}; \tag{22}$$

$$\{\Omega\} \overset{\Delta}{=} \begin{Bmatrix} \{\theta\} \\ \{\dot{\theta}\} \end{Bmatrix} \qquad \text{State vector, } \in \Re^{2n}; \tag{23}$$

$$\{\Gamma\} \overset{\Delta}{=} -(\{C\} + \{G\} + \{F\}) \qquad \text{Non-linear terms of the model of the robot} \tag{24}$$

By admitting that the uncertainties are null, Equation (25) defines a control law that includes terms of the dynamic model of the robot and the reference model.

$$\{\tau\} = ([D][B]^{-1}[\underline{B}]\{u\} + [D][[A_1] \quad [A_2]]\{\Omega\} - \{\Gamma\}) + \{\Delta\} \tag{25}$$

Using Eq. (20) into (25) results:

$$\{\dot{\Omega}\} = ([A] + [B][[A_1] \quad [A_2]])\{\Omega\} + [\underline{B}]\{u\}$$

$$\{\dot{\Omega}\} = [\underline{A}]\{\Omega\} + [\underline{B}]\{u\} \tag{26}$$

Equation (26) describes a linear, stable and not-connected model. The error of tracking is defined as mathematical difference between equations (26) and (14):

$$\{\dot{e}\} = [\underline{A}]\{e\} \tag{27}$$

Where:

$$\{e\} \overset{\Delta}{=} \{\Omega\} - \{\underline{\Omega}\} \tag{28}$$

By analyzing Eq. (27), the asymptotic tracking is guaranteed by an adequate choice of the matrix associated with the state vector for the reference model. However, it is necessary the full knowledge of the dynamics of the plant to be controlled, in order to make it possible to cancel the nonlinear effect of the model.

4.1.3 Inclusion of the parametric uncertainties

The full knowledge about a dynamic model is restrictive enough to the practical application. Thus, the related parametric uncertainties to Eq. (20) are admitted, which disables the exact cancellation of this term. Thus, Eq. (25) can assume the following form (Ge, et al., 1998).

$$\{\tau\} = \{\hat{\tau}_M\} + \{\tau_R\} \tag{29}$$

Where:

$$\{\hat{\tau}_M\} \overset{\Delta}{=} \left([D][B]^{-1}[\underline{B}]\{u\} + [D][[A_1] \quad [A_2]]\{\Omega\} - \{\hat{\Gamma}\}\right) + \{\Delta\} \quad \text{Term based on the model;} \tag{30}$$

$$\{\tau_R\} \overset{\Delta}{=} -[\kappa]sgn(\{e\}) \qquad\qquad\qquad \text{Robust term;} \tag{31}$$

$$\{\hat{\Gamma}\} \overset{\Delta}{=} [v]^T\{\rho\} + \{\varepsilon\} \qquad\qquad\qquad \text{Estimated term;} \tag{32}$$

$[v]$ Regression matrix;

$\{\rho\}$ Parameters vector;

$\{\varepsilon\}$ Error of estimation;

$\{\kappa\}$ Gain vector;

$sgn(\bullet)$ Signal function;

$\{e\}$ Error of the model

Using Eq. (20) into Eq. (29) results:

$$\{\dot{\Omega}\} = [A]\{\Omega\} + \{B\}[D]^{-1}\left(\{\hat{\tau}_M\} + \{\tau_R\} + \{\Gamma\}\right) \tag{33}$$

Using Eq. (33) into Eq. (31) follows:

$$\{\dot{\Omega}\} = \left([A] + [B][[A_1] \quad [A_2]]\right)\{\Omega\} + [\underline{B}]\{u\} + [B][D]^{-1}\left(\{\tau_R\} + \{\Gamma\} - \{\hat{\Gamma}\}\right)$$

$$\{\dot{\Omega}\} = [\underline{A}]\{\Omega\} + [\underline{B}]\{u\} + [B][D]^{-1}\left(\{\tau_R\} + \{\hat{\Delta}_\Gamma\}\right) \tag{34}$$

The mathematical difference between equations (34) and (14) is:

$$\{\dot{e}\} = [\underline{A}]\{e\} + [B][D]^{-1}\left(\{\tau_R\} + \{\hat{\Delta}_\Gamma\}\right) \tag{35}$$

Analyzing Eq. (35), we can conclude that the objective of the τ_R term is to suppress the error in the process of identification of the estimated term (Eq. 32).

Equation (32) is constructed by using the Radial Basis Function (RBF) Neural Network, which enables nonlinear mapping. The adaptability of its parameters can guarantee the stability of the control system in a closed loop, in the Lyapunov sense. Equation (36) can gives the estimated term vector.

$$\{\hat{\Delta}_\Gamma\} = \begin{bmatrix} \{\hat{\Delta}_{\Gamma 1}\} \\ \{\hat{\Delta}_{\Gamma 2}\} \\ \vdots \\ \{\hat{\Delta}_{\Gamma n}\} \end{bmatrix} \equiv \begin{bmatrix} [v_1]^T\{\rho\} \\ [v_2]^T\{\rho\} \\ \vdots \\ [v_n]^T\{\rho\} \end{bmatrix} + \begin{bmatrix} \{\varepsilon_1\} \\ \{\varepsilon_2\} \\ \vdots \\ \{\varepsilon_n\} \end{bmatrix} = \{v\}^T \bullet \{\rho\} + \{\Xi\} \tag{36}$$

Where the k-th component is:

$$\{\hat{\Delta}_{\Gamma k}\} = \begin{bmatrix} I & v_1 & \cdots & v_m \end{bmatrix} \begin{bmatrix} v_k \\ \rho_1 \\ \vdots \\ \rho_m \end{bmatrix} + \varepsilon_k \equiv [v_k]^T\{\rho\} + \varepsilon_k \tag{37}$$

According to GE *et al*. (1998), the stability in the Lyapunov sense can be assured by rewriting Eq. (35), using Eq. (36).

$$\{\dot{e}\} = [A]\{e\} + [B][D]^{-1}\{\{v\}^T \bullet \{\rho\}\} + [B][D]^{-1}\{\Xi\} + [B][D]^{-1}\{\tau_R\} \tag{38}$$

Lets us consider the following Lyapunov function:

$$V(e,v) = \{e\}^T[P]\{e\} + \sum_{i=1}^{n}\{v\}_i^T[\Pi]_i^{-1}\{v\}_i \tag{39}$$

Where:

$[P]=[P]^T$	Solution of the Lyapunov equation: $[A]^T[P]+[P][A]=-[Q]$;	(40)
$[\Pi]_i$	Constant matrix definite positive	(41)

Taking the time derivative of the Eq. (39) and using Eq. (38) results:

$$\dot{V}(\{e\},\{v\}) = 2\{e\}^T[P]\left([A]\{e\} + [B][D]^{-1}\{\{v\}^T \bullet \{\rho\}\} + [B][\;]^{-1}\{\Xi\} + [B][D]^{-1}[\tau_R]\right) + 2\sum_{i=1}^{n}\{v\}_i^T[\Pi]_i^{-1}\{\dot{v}\}_i \tag{42}$$

According to Eq. (42), Eq. (43) is the adaptability law for the parameters of the RBF net, which assures the stability in closed loop.

$$\{\dot{v}\}_i = -[\Pi]_i\{\rho\}_i\{e\}^T[P]\{b\}_i[D]^{-1} \tag{43}$$

Using Eq. (42) into Eq. (43) results:

$$\dot{V}(e,v) = 2\{e\}^T[P][A]\{e\} + 2\{e\}^T[P][B][D]^{-1}(\{\Xi\} + \{\tau_R\}) \tag{44}$$

Using Eq. (31) and Eq. (40) to rewrite Eq. (44) results:

$$\dot{V}(e,v) = -\{e\}^T[Q]\{e\} + 2\{e\}^T[P][B][D]^{-1}\left(\{\Xi\} - [k]sgn\left(\{e\}^T[P][B][M]^{-1}\right)\right) \tag{45}$$

The matrixes [P] and [B] are definite positive and [D] is a non-singular matrix. Equation (45) is definite negative if the components of matrix **[k]** are chosen according to Eq. (46).

$$k_{ii} \geq \left|\hat{\Delta}_{\Gamma i}\right| \tag{46}$$

So:

$$\dot{V}(e,v) = -\{e\}^T[Q]\{e\} - 2\left\|[e]^T[P][B][D]^{-1}\right\| < 0 \qquad (47)$$

4.2 The automatic generator trajectories of the trunk

Commonly, the biped walking robot is endowed with a trunk (inverted pendulum) to compensate the inertial and gravitational forces intrinsic to the dynamic gait. However, this addition causes inherent problems to the stability. First, there is the problem to keep the trunk under control in the vertical position, which can be solved by employing a servomechanism, as presented in section 4.1. The second problem is related to the generation of trunk's trajectory that can assure postural stability. It is worthy to consider the dynamic of the contact between the support foot and the ground. The ZMP criterion can provide a system of nonlinear dynamic equations to obtain the trajectories of the trunk (Takanishi, 1989).

The second problem was solved by Gonçalves and Zampieri (2003), who employed a recurrent neural network (RNN) to generate the trajectories of the trunk in the automatic form, based on the ZMP criterion. An identification scheme was presented to obtain the parameters vector of the RNN, utilizing a first-order standard back-propagation with momentum. This way, a compensative trunk motion makes the actual ZMP get closer to the planned ZMP.

Here, we utilized the same scheme, using an RNN with 2 intermediate layers, and 20 neurons in each layer. The stop criterion was **0.0001** m that is the mean-square error between the actual ZMP and the planned ZMP.

5. Simulations and Results

The biped walking robot was divided in two subsystems: trunk (inverted pendulum) and the legs. The dynamic model of the biped walking robot is defined by equations (2), (3) and (4). These equations were implemented in Matlab/Simulink®, by using the S-functions (Harman, T. L. and Dabney, J. B., 2003). Figure 3 illustrated the disturbances caused by the trunk in the legs (Disturbance-Trunk) and vice versa (Disturbance-Legs). The connection named "u-trunk" receives the trajectories of the trunk from the generator of trajectories for the trunk. The connection "u-legs" receives the planned gait from the gait automatic generator.
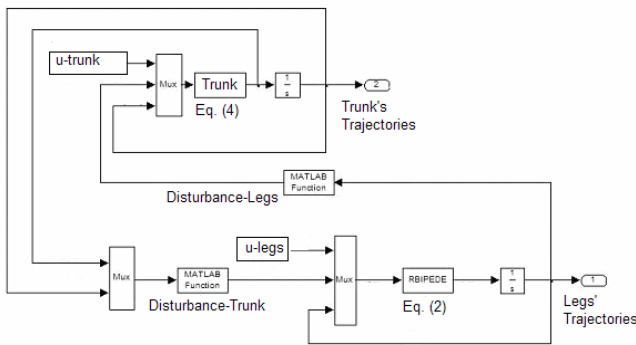
Figure 3. The biped walking model implementation.　　　Figure 4. Implementation of the integrate control system.
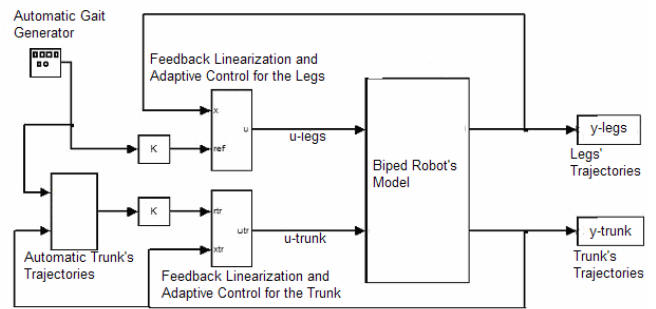
Figure 4 illustrates the integrated control system for the biped walking robot. The block "Biped-Model" contains the models of the subsystems and the disturbances. The adaptive control systems for the trunk (ACS-Trunk) and for the legs (ACS-Legs), in despite of independent, are similar. They receive the angular signals of position and speeds that are compared with the corresponding trajectories planned by the gait automatic generator. The automatic generator of trajectories for the trunk receives the angular signals of position and speeds from both subsystems, to compose the input signals to the RNN.

For the simulation, we utilized a gait with the following characteristics: the pelvis remains parallel in relation to the ground, the step length is **0.17** m, the speed walking is **0.55** m/s, the angle between the foot and the ground is **0.2** rad and the maximum height for the balancing foot is **0.0386** m. The total time to complete a step is **0.9** s. Twenty percent of this time is expended in the bi-support phase.

For this gait characteristic, the angular positions were computed by using inverse kinematics techniques, and the speeds, by employing Jacobian computation. The results were presented in Fig. 5 and Fig. 6 that describe the angular and the velocity trajectories for the first (θ_1), second (θ_2), third (θ_3) joints, and so on.
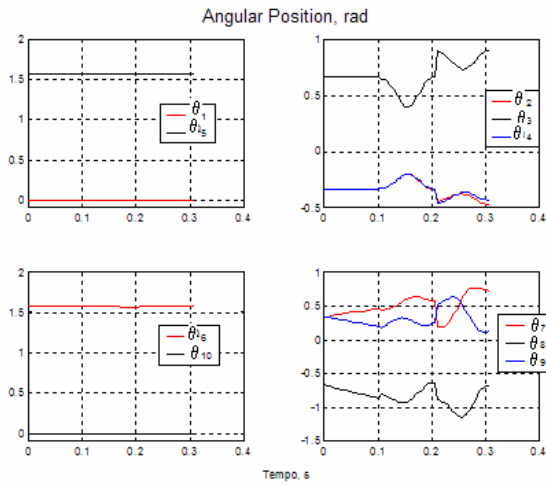
Figure 5. Angular position for the legs.
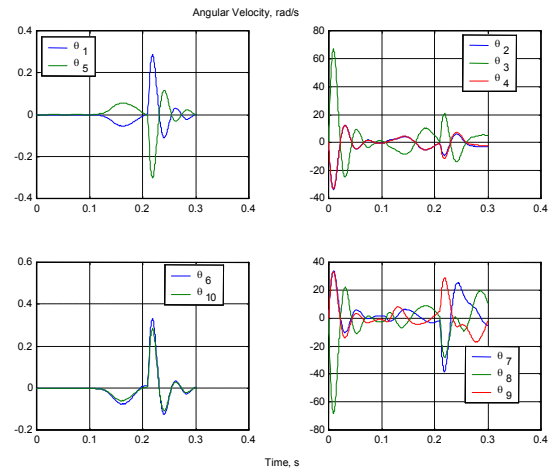
Figure 6. Angular velocities for the legs.

Figure 7 shows the trajectories for the angular position and velocity of the trunk that were used for the reference of the trunk. The RNN decides the problem of the angular positioning the trunk and the angular velocities the trunk are decided from the reference model.

Figure 8 shows the tracking errors obtained from the control system of the trunk. The angular position error is around the ± **1.5×10⁻³** rad and presents a decreased oscillatory behavior. The corresponding angular speeds present similar behavior.
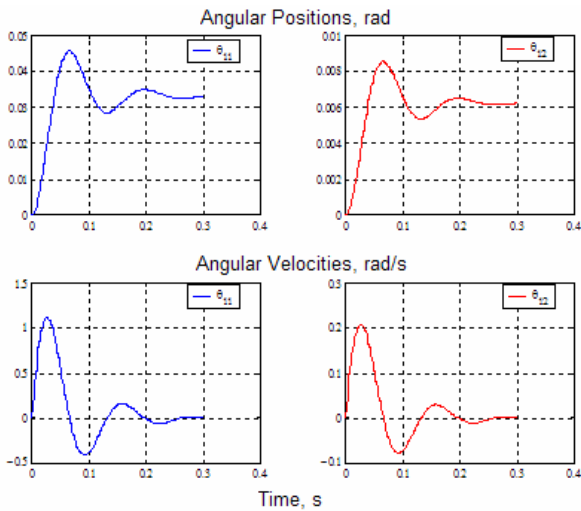
Figure 7. Reference signals for the trunk.
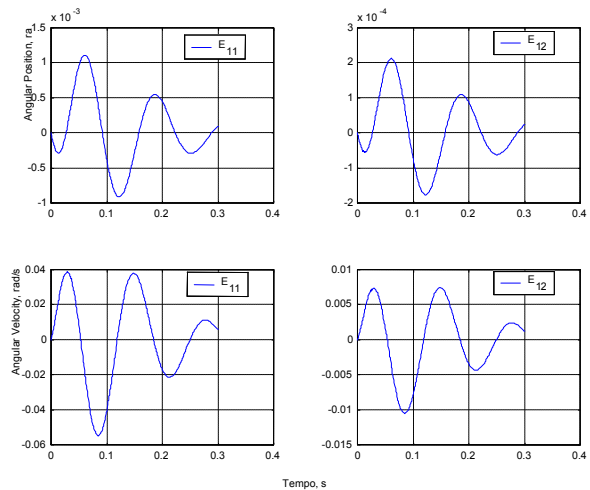
Figure 8. Tracking errors for the trunk.

Figures 9 and 10 present the corresponding errors ($E_j = \theta_j - \underline{\theta}_j$) of tracking of the position and the velocities associates to the legs, respectively. The angular position errors are limited around **0.06** rad in the beginning of the movement, reaching around **0.02** rad in approximately **0.1** s and around **zero** rad after **0.2** s (with exception of the balancing leg). Similar behavior is verified for the corresponding velocity errors.
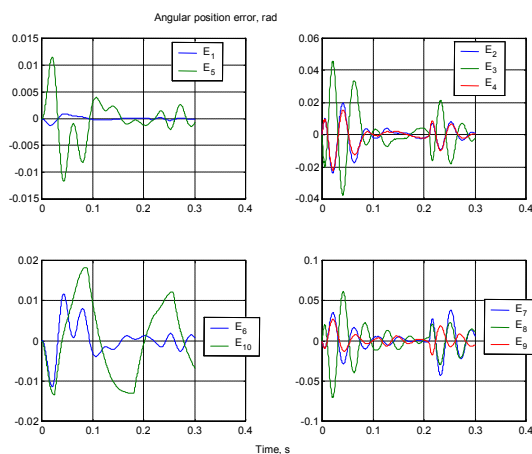
Figure 9. Tracking error of the legs' position.
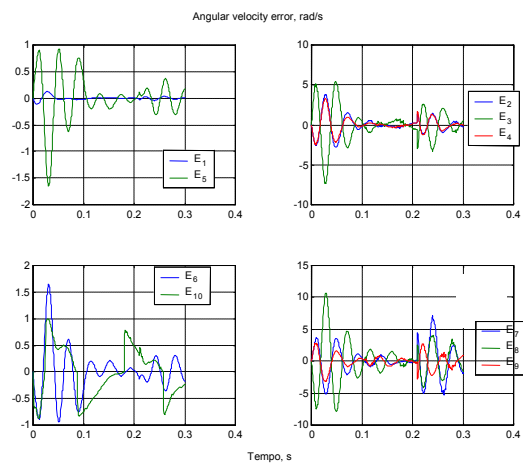
Figure 10. Tracking error of the legs' velocity.

6. Conclusions and Comments

This work aimed at contributing to the area of biped walking robots that explore the dynamic gait. A biped walking robot endowed with trunk was conceived, composed by a chain of rigid links interconnected by rotating joints, totalizing twelve joints that enable positioning in the three-dimensional space. For the symbolic modeling, we implemented the formalism of Newton-Euler in the environment of Maple®, offering an automatic symbolic modeler.

We projected and implemented the integrated control system. The control law includes terms of the dynamic model of the robot, of the reference model and of the uncertainties. An RBF neural network was used for the on-line identification of the parametric uncertainties. An automatic gait generator, adaptable to the local conditions of the land, was conceived and implemented, functioning perfectly in terms of passage speed, length of the step and maximum height for the foot in balance. After planning the gait, the trajectory for the trunk was determined by a RNN, integrated to the control system, which could update the angular positioning of the trunk from the evolution of the legs. The system of control and the automatic generator of trajectories for the trunk constitute adaptive mechanisms, developed to solve the dynamic gait control.

In the simulation, we synthesized a gait for the robot with similar requirements to those of the human being gait, with a walking speed of **2** km/h. By using the inverse kinematics computation, the corresponding angular position was computed. The angular speeds were computed by using Jacobian matrix, as shown in Fig. 5 and Fig. 6.

The integrated control system presents a steady behavior and, besides tracking signals of reference for the legs and for the trunk, allows to reject the disturbances caused by the coupling between the legs and trunk.

7. References

GE, S. S., Lee, T. H. and Harris, C. J., 1998, "Adaptive Neural Networks Control of Robotic Manipulator." World Scientific Series in Robotics and Intelligent Systems, Vol. 19, 381 p.

Geddes, K., Monagan, M. B. and Springer-Velarg, 1997, "Maple V Programming Guide." Ed. Springer-Verlag NY. 379p.

Gonçalves, J. B. and Zampieri, D. E., 2003, "Recurrent Neural Network Approaches for Biped Walking Robot based on Zero-Moment-Point Criterion." RBCM - J. of. the Brazilian Soc. Mechanical Sciences, Vol. XXV. pp 53-62.

Goswami, A., 1999, "Postural Stability of Biped Robots and the Foot-Rotation Indicator (FRI) Point". The International Journal of Robotics Research, Vol. 18, No. 6, pp. 523-533.

Harman, T. and Dabney, J. B., 2003, "Mastering Simulink". Ed. Prentice-Hall. 400 p.

Li, Q., Takanishi, A., and Kato, I., 1992, "Learning Control of Compesative Trunk Motion for Biped Walking Robot based on ZMP criterion." In Proceedings of the 1992, IEEE/RSJ International Conference on Intelligent Robots and System. Raleigh, NC.

Predabon, E. and Bocchese, C., 2003, "SolidWorks 2004 – Projeto e Desenvolvimento". Ed. Érica. 408 p.

Takanashi, A., 1989, "Robot Biped Walking Stabilized with Trunk Motion." Proceedings of ARW on Robotics and Biological System.

8. Responsibility notice

The authors are the only responsible for the printed material included in this paper.